DOI:10.1021/jf100613x

JOURNAL OF AGRICULTURAL AND FOOD CHEMISTRY
ARTICLE

Allyl Sulfides Inhibit Cell Growth of Skin Cancer Cells through Induction of DNA Damage Mediated G_2/M Arrest and Apoptosis

Hsiao–Chi Wang,[†] Jen-Hung Yang,[‡] Shu-Chen Hsieh,[†] and Lee-Yan Sheen*,[†]

[†]Graduate Institute of Food Science and Technology, National Taiwan University, No. 1, Sec. 4, Roosevelt Road, Taipei 106, Taiwan, and [‡]Department of Dermatology, Chung Shan Medical University Hospital, and School of Medicine, Chung Shan Medical University, No.110, Sec.1, Jianguo North Road, Taichung 402, Taiwan

Diallyl sulfide (DAS), diallyl disulfide (DADS), and diallyl trisulfide (DATS), extracted from crushed garlic by steam-distillation, have been reported to provide the anticancer activity in several cancer types. However, their mechanisms of effects on skin cancer cells remain unclear. Therefore, we used human melanoma A375 cells and basal cell carcinoma cells as the models to elucidate the effects of these three allyl sulfides. Basal cell carcinoma (BCC) is known to be the most prevalent type of skin cancer, and melanoma is the most lethal form. We found that DATS revealed better growth inhibition of A375 and BCC cells than DADS and DAS did. We further demonstrated that DATS increased intracellular reactive oxygen species (ROS) generation, induced cytosolic Ca^{2+} mobilization, and decreased mitochondrial membrane potential ($\Delta\Psi m$). Western blot results showed the concordance for the expression of molecules involved in G_2/M arrest and apoptosis observed by cell cycle and cell viability analysis. Moreover, we detected the activation of p53 pathway in response to the oxidative DNA damage. DATS also displayed selective target of growth inhibition between skin cancer cells and normal keratinocyte HaCaT cells. Taken together, these results suggest that DATS is a potential anticancer compound for skin cancer.

KEYWORDS: Skin cancer; basal cell carcinoma; melanoma; allyl sulfides; DNA damage; cell cycle; apoptosis

INTRODUCTION

Skin cancer is the most frequent cancer in the western population, including melanoma and nonmelanoma skin cancer (*1*). Each year there are more new cases of skin cancer than the combined incidence of cancers of the breast, prostate, lung, and colon in the United States (*2*). Epidemiological studies indicated that the morbidity rate of skin tumors is rising with an increasing age range over the past decades in Asia (*3*, *4*). Basal cell carcinoma (BCC) is the most common type of nonmelanoma skin cancer, which constitutes more than 80% of skin cancers (*1*). BCC is a keratinocyte tumor derived from basal layer of skin tissue, exhibiting slow growth rate and rarely spread (*5*). In contrast, melanoma is the least common type but accounts for 80% deaths of skin cancer. Malignant melanoma has been characterized by a strong tendency to develop metastasis and resistant to chemotherapy (*6*). Many evidence indicated that ozone depletion, excessive ultraviolet light exposure, dietary factor, and lifestyle are associated with the development of skin cancer (*1*). Therefore, it is important to develop more preventive and therapeutic strategies for skin cancer.

Dietary intake of *Allium* vegetables, such as garlic, may play a role in reducing the risk of certain cancers (*7*). Allyl sulfides, the important organosulfur components of garlic oil, have been reported to suppress the growth of multiple cancer cells in culture and in vivo models (*8*−*10*). Diallyl sulfide (DAS), diallyl disulfide (DADS), and diallyl trisulfide (DATS) are most abundant in garlic oil (*11*). The number of sulfur atoms on allyl sulfides determines their biological activity such as anticancer and anti-inflammatory effects (*12*, *13*). Our previous study revealed that the cell cycle arrested ability increased as the number of sulfur atoms on allyl sulfides increased in human J5 hepatoma cells (*9*). The anticancer effect of allyl sulfides is associated with suppression of cell proliferation, inhibition of angiogenesis, and induction of cell cycle arrest and mitochondrial apoptotic pathway (*8*, *10*, *14*). Allyl sulfides have been shown to produce ROS via disulfide bond cleavage involved in their antiproliferative activity on cancer cells (*15*). Moreover, induction of ROS generation and cytosolic Ca^{2+} influx by allyl sulfides have played important roles in activation of cell cycle arrest and endoplasmic reticulum (ER) stress-mediated apoptosis (*8*). Interestingly, numerous researchers focused on the antitumorigenesis effect of allyl sulfides in animal model of skin carcinogenesis. Studies have shown that DAS prevented chemically induced skin tumor via decreasing COX-2 expression, increasing p53 and $p21^{wafl/cip}$ expressions, and inducing apoptosis (*16*, *17*). Among these allyl compounds, DATS has been reported to be the most potent in inhibiting carcinogen-induced tumor promotion (*18*). However, there is little research related the effect and molecular mechanism of allyl sulfides on the cell models of human skin cancer.

*To whom correspondence should be addressed. Phone: 886-2-3366-4129. Fax: 886-2-2362-0849. E-mail: lysheen@ntu.edu.tw.

 Published on Web 05/11/2010 © 2010 American Chemical Society

Recent evidence suggested that DNA damage agent with less normal tissue toxicity is one of the newest cancer therapies. Human tumors frequently have defects in response to DNA damage, including cell cycle checkpoints, histone modifications, and DNA repair, compared with normal human cells (*19*). DNA damage induced p53-caspase-dependent and independent pathways, e.g., postmitotic cell death or cell division arrest, have been found providing antiproliferative effect during chemotherapy. Histone H_2AX phosphorylation is a rapid and sensitive cellular response to DNA damage, and H_2AX phosphorylated on serine 139 (γ-H_2AX) is also linked to apoptosis (*20*). In this study, we clarified the anticancer effect of these three allyl sulfides using human skin cancer cells with special emphasis on its underlying mechanisms of DNA damage signaling pathway.

MATERIALS AND METHODS

Materials and Chemicals. DAS (purity ≥97%), DADS (purity ~80%) and DATS (purity ≥98%) were purchased from Fluka Chemical (Buchs, Switzerland), Toyo Kasei Chemical (Tokyo, Japan), and LKT Laboratories (St. Paul, MN), respectively. Dulbecco's modified Eagle medium (DMEM), RPMI 1640 medium, fetal bovine serum (FBS), trypsin-EDTA, and antibiotic−antimycotic solution were purchased from Gibco Laboratories (Grand Island, NY). In addition, Bradford protein assay was obtained from Bio-Rad Laboratories (Hercules, CA). The primary antibodies: anti-phospho-γ-H_2AX (Ser 139), anti-phospho-γ-p53 (Ser15), anti-$p21^{waf1/cip1}$, anti-cyclinB_1, anti-cdc25c, anti-cdc2, anti-Wee 1, anti-poly-(ADP-ribose) polymerase (PARP), anti-caspase-3, anti-caspase-9, anti-β-actin, and anti-rabbit or anti-mouse IgG horseradish peroxidase (HRP)-linked secondary antibodies were purchased from Cell Signaling Technology (Danvers, MA). ECL chemiluminescence reagent for Western blot was obtained from Millipore (Billerica, MA). All other chemicals were obtained from Sigma-Aldrich with analytical or reagent grade products.

Cell Culture and Cell Treatment. The human melanoma A375 cell line, basal cell carcinoma (BCC) cell line, and human keratinocyte HaCaT cell line were obtained from Professor Jen-Hung Yang (Department of Dermatology, Chung Shan Medical University Hospital, Taiwan). A375 ce1ls were cultured in DMDM, whereas BCC and HaCaT cells were cultured in RPMI 1640 medium. The cells were cultured in complete medium (pH 7.3−7.4) at 37 °C, 5% CO_2, and 90% relative humidity. Culture medium was supplemented with 10% of FBS and 1% of antibiotic−antimycotic solution. Allyl sulfides were diluted in sterile dimethyl sulfoxide (DMSO, Sigma) before addition to cultures. Control cultures were treated with 0.2% DMSO.

Cell Viability Analysis. Cell viability was determined using MTT assay as described previously (*21*). Cells (5×10^3 cells/100 μL/well) were seeded in 96-well plates for 24 h. After 24 h of incubation, cells were treated with 100 μL serum-free medium containing different concentrations of DAS, DADS, and DATS for 24 and 48 h. At the end of the stipulated period, MTT solution (5 mg/mL) was added to each well for 4 h of incubation. The resulting formazan was dissolved in DMSO and the absorbance recorded at 570 nm using BioTek plate reader (Winooski, VT). The cells which were treated with 0.2% DMSO were served as control of 100% survival.

Cell Cycle Distribution Assay. Cell cycle distribution was analyzed by FACScan flow cytometry (Becton Dickinson, San Jose, CA) equipped with CellQuest software. Briefly, cells (1.15×10^4 cells/cm^2) were cultured in a 6 cm dish and treated with 25 μM of DAS, DADS, and DATS for 24 h. Cells were fixed by 70% ice-cold ethanol at −20 °C overnight and then washed with ice-cold PBS. The resulting solution was incubated with RNase (1 mg/mL), propidium iodide (4 μg/mL), and Triton X-100 (0.1%) at room temperature for 30 min. Subsequently, cells were filtered before analyzed by flow cytometry equipped with an argon laser at 488 nm wavelength (*22*). A minimum of 10000 cells per sample were collected, and the cell cycle distribution was determined by ModFit LT version 2.0 software (Verity Software House, Topsham, ME) to calculate the percentages of cells in each phase.

Intracellular ROS Generation, Cytosolic Ca^{2+} Concentration, and Mitochondrial Membrane Potential ($\Delta\Psi m$) Determination. The levels of ROS, Ca^{2+} and $\Delta\Psi m$ were examined by flow cytometry using carboxyl-H_2DCFDA, Fluo-3/AM (Invitogen), and $DiOC_6$ (Sigma), respectively. Cells (1.15×10^4 cells/cm^2) were treated with 25 μM of DAS, DADS, and DATS for 1 h to detect the changes of ROS and Ca^{2+} level. In addition, $\Delta\Psi m$ level of A375 and BCC cells was performed after DATS treatment for 24 h. The cells were harvested and washed twice, separately resuspended in 500 μL of carboxyl-H_2DCFDA (10 μM), Fluo-3/AM (5 μM), or $DiOC_6$ (4 μM) at 37 °C for 30 min. Stained cells were washed, resuspended in 500 μL PBS, and used for flow cytometry analysis. Mean fluorescence intensity (MFI) detected by FLl channel was analyzed using CellQuest software (*23*).

Western Blot Analysis. Western blotting was carried out as described previously study (*9*). Cells (1.15×10^4 cells/cm^2) were treated with test compounds at different time points. Total cell extracts were prepared in

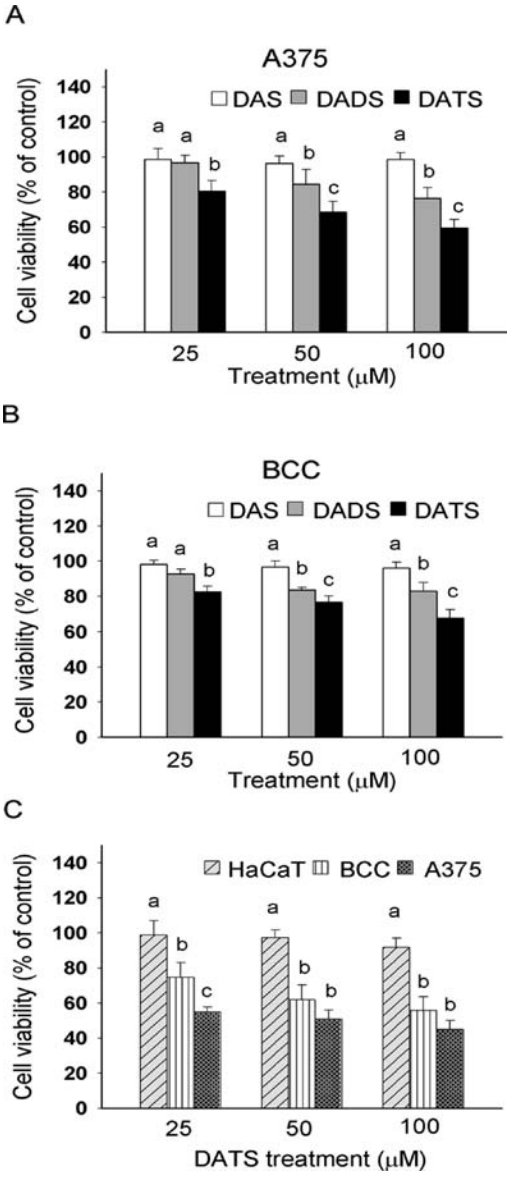

Figure 1. Effect of allyl sulfides on cell viability of A375, BCC, and HaCaT cells. A375 cells (**A**) and BCC cells (**B**) seeded in 96-wells plates were treated with control, DAS, DADS, or DATS at the dose indicated for 24 h, respectively. (**C**) A375, BCC, and HaCaT cells were incubated either in the absence or presence of DATS at various concentrations for 48 h. Cell viability was determined by MTT assay as described in Materials and Methods. Data are expressed as the relative percentage to control. Results are mean ± SD from three independent experiments and analyzed statistically using ANOVA and Duncan's test. Different letters (a−c) represent statistically significant differences among treatments, $p < 0.05$.

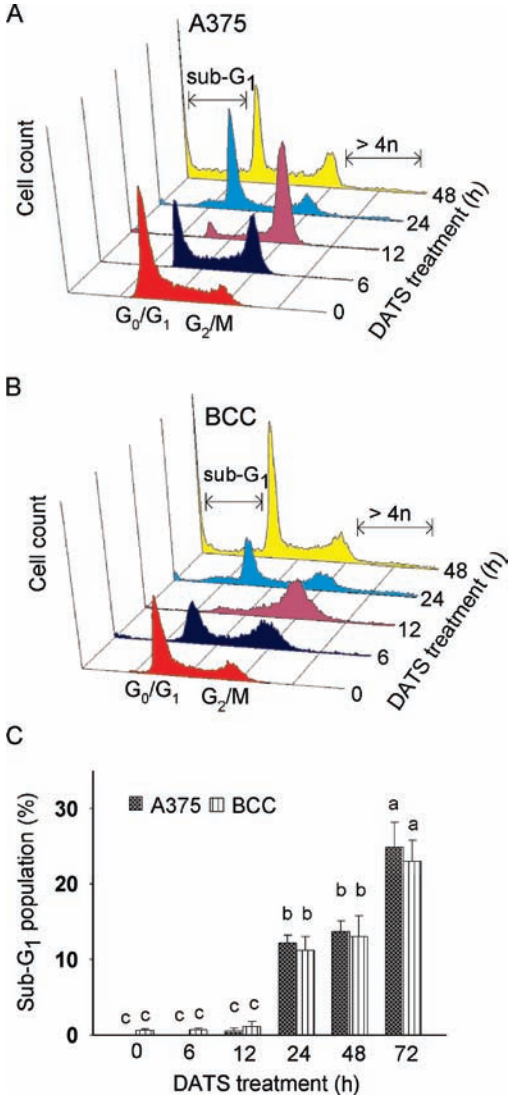

Figure 2. Time course analysis of cell cycle progression in A375 and BCC cells after the exposure of DATS. Cells were treated with 25 μM of DATS and subjected to flow cytometry analysis at the indicated time periods. The cycle distribution was revealed at the two major peaks as G_0/G_1 and G_2/M based the DNA content. Cells with G_2/M arrest and polyploidy (the DNA content over 4*n*) in A375 cells (**A**) and BCC cells (**B**) were shown. The percentage of sub-G_1 population shown in (**C**) is mean ± SD of three independent experiments. Different letters (a−c) represent statistically significant differences among treatments, $p < 0.05$.

ice-cold RIPA lysis buffer (1% NP-40, 1 mM PMSF, 10 μg/mL aprotinin, 100 mM sodium orthovanadate, 0.5% Triton X-100). The cell lysates were sonicated and cleared by centrifugation, and the protein concentration in the lysates was measured by Lowry's method (*24*). Protein (50 μg) was loaded over 12% or 15% SDS-PAGE gels, transferred to PVDF membranes, blotted with specific primary antibodies respectively, and then labeled by HRP-conjugated secondary antibody according to the manufacturer's instructions. The membranes were performed using the enhanced ECL chemiluminescence Western blotting detection system. Equal loading was confirmed by reprobing the membrane with β-actin. The relative density of each band after normalization for β-actin was shown under each band as a fold-change compared with control.

Statistical Analysis. All experiments were performed in triplicate and presented as mean ± SD. Statistical analyses were performed using one-way analysis of variance (ANOVA) and Duncan's multiple comparison tests (SAS Institute Inc., Cary, NC) to determine significant differences among means of treatments ($p < 0.05$).

Table 1. Effect of Allyl Sulfides on Cycle Distribution in A375 and BCC Cells[a]

			phase of cell population (%)[a]		
cells	treatment	sub G_1 (%)	G_0/G_1	S	G_2/M
A375	control	1.5 ± 0.9 b	75.2 ± 3.6 a	21.3 ± 3.2 b	3.5 ± 0.7 b
	DAS	2.8 ± 1.9 b	79.4 ± 1.3 a	17.2 ± 0.7 b	3.4 ± 0.5 b
	DADS	4.2 ± 1.4 b	73.6 ± 4.5 a	22.2 ± 1.7 ab	4.2 ± 1.4 b
	DATS	9.9 ± 2.8 a	57.2 ± 3.2 b	26.8 ± 2.1 a	16.0 ± 2.8 a
BCC	control	3.1 ± 0.6 b	47.3 ± 3.7 ab	39.6 ± 6.2 ab	13.1 ± 0.6 b
	DAS	2.9 ± 0.4 b	57.5 ± 2.7 a	34.9 ± 1.3 b	7.6 ± 0.6 b
	DADS	4.0 ± 0.6 b	43.8 ± 1.2 ab	45.7 ± 3.8 a	10.5 ± 1.6 b
	DATS	12.9 ± 3.1a	40.3 ± 7.3 b	36.7 ± 3.2 b	23.0 ± 4.4 a

[a] Cells were treated with control and 25 μM of DAS, DADS, or DATS for 24 h. Then, cells were harvested and stained with propidium iodide as described in Materials and Methods. Data are expressed as mean ± SD of three determinations and analyzed statistically using ANOVA and Duncan's test. Different letters (a−b) represent statistically significant differences in the same column among treatments, $p < 0.05$.

RESULTS

DATS was More Effective Than DADS and DAS in Decreasing Cell Viability of A375 and BCC Cells. To address the effects of allyl sulfides on the cell viability of skin cancer cells, we used A375 and BCC cells as models and employed MTT as an assay system to analyze the effect of DAS, DADS, and DATS. As shown in **Figure 1A**,**B**, none of the concentration of DAS we applied in either A375 or BCC exhibited the killing effect, while DADS and DATS revealed a dose dependent efficiency in suppressing the survival rates in both cell lines. When compared with the other two allyl sulfides, DATS had the greatest effects on the inhibition of cell viability. Although DAS did not show any effect at 24 h treatment, it significantly suppressed cell viability at 48 h (data not shown). In addition, DATS decreased the percentage of cell viability in dose and time-dependent manner and also caused the morphology change of A375 and BCC cells, including cell floating and cell shrinkage (data not shown). To further confirm DATS-mediated growth inhibition is cancer cell specific, we investigated the cytotoxicity of DATS on normal cells. As revealed in **Figure 1C**, the viability of HaCaT cells, a normal skin cell line, was not affected in the presence of DATS at the dose we applied up to 48 h. This finding was significantly different from its effect on skin cancer cells, indicating DATS exerted its survival inhibition specifically in skin cancer cells instead of normal skin cells.

DATS Caused G_2/M Arrest in A375 and BCC Cells. On the basis of the growth inhibitory effect of DATS in A375 and BCC cells, we next examined its effect on cell cycle using 25 μM of DATS at different time points. As summarized in **Figure 2A**,**B**, both A375 and BCC cells displayed G_2/M arrest as early as 6 h after exposure to DATS. After 12 h of treatment, DATS induced 5−7-fold G_2/M percentage in A375 cells (61.7 ± 9.7%) and BCC cells (68.9 ± 2.5%) compared to that of A375 cells (8.3 ± 2.9%) and BCC cells (12.9 ± 0.4%) at 0 h. In addition, DATS increased the G_2/M cell distribution and sub-G_1 population throughout the time points we examined (**Figure 2C**). Interestingly, when compared with the control, both cell lines displayed G_2/M arrest accompanied by an increase of ploydiploid DNA (> 4*n*) after exposure to DATS (**Figure 2**A and **2**B). DATS caused G_2/M arrest approximately increased by 4.5-fold in A375 cells and 2-fold in BCC cells at 24 h. In contrast, neither DAS nor DADS at the same concentration showed any effect on cell cycle distribution (**Table 1**). The level of growth inhibition in A375 and BCC cells among allyl sulfides treatment were correlated with the degrees of G_2/M arrest and apoptosis evoked by the treatments.

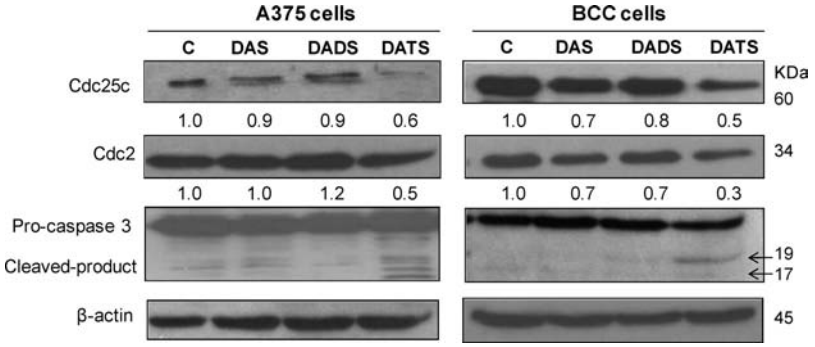

Figure 3. Protein expressions of Cdc25c, Cdc2, and caspase-3 in allyl sulfides treated A375 and BCC cells. Cells were treated with control (C) and 25 μM of DAS, DADS, or DATS for 24 h. Cell lysates were subjected to immunoblot analysis using specific antibodies for Cdc25c, Cdc2, and the cleavage forms of caspase-3 (pointed by the arrows) were examined. Here β-actin was detected as the internal standard control. Quantification of protein levels by β-actin-normalized densitometry is shown on the bottom of each band. Immunoblotting for each protein was done at least twice using independently prepared lysates.

DATS Induced Cell Cycle Arrest and Apoptosis via Inhibition of Cdc25c, Cdc2 Protein Level and Activation of Caspase-3. Because DATS consistently induced alteration in cell cycle progression, we further scrutinized whether the expression of G_2/M modulators such as Cdc25c phosphatases (Cdc25c) and cyclin-dependent kinase (CDK, Cdc2) were influenced by allyl sulfides. Results of Western blot showed that 25 μM of DATS decreased the protein levels of Cdc25c and Cdc 2 compared with those of control in A375 and BCC cells after 24 h treatment. Moreover, the protein level of cleaved caspase-3, a marker of cell apoptosis, was increased by DATS in A375 and BCC cells. However, DAS and DADS did not show any effect on these proteins at the same concentration (**Figure 3**).

Effect of DATS on The Levels of ROS Generation, Ca^{2+} Mobilization and Mitochondrial Membrane Potential ($\Delta\Psi m$). Growing evidence indicated that ROS and ER stress play an important role in allyl sulfides mediated apoptosis (*8*). Disruption of calcium homeostasis in various cell types is a well-known marker of ER stress (*25*). To explore the induction of intracellular ROS generation and cytosolic Ca^{2+} mobilization by these three allyl sulfides, we used the probes carboxy-H_2DCFDA and Fluo-3/AM to analyze ROS and Ca^{2+} in A375 and BCC cells, respectively. Moreover, we quantified the mean fluorescence intensity (MFI) of cells stained with carboxy-H_2DCFDA and Fluo-3/AM by CellQuest software. Our result revealed that DATS significantly increased intracellular ROS generation in both A375 cells (54.7 ± 4.9) and BCC cells (60.7 ± 5.0) compared to those of the control (A375 cells: 27.0 ± 4.0; BCC cells: 37.4 ± 4.3), while DAS and DADS slightly induced intracellular ROS formation in A375 and BCC cells without any statistical significance (**Figure 4A**). Similar results could be observed in the estimation of Ca^{2+} concentration in the cell lines we investigated. As exhibited in **Figure 4B**, DATS significantly increased Ca^{2+} concentration in A375 cells (47.1 ± 5.9) and BCC cells (41.6 ± 9.6) as compared with control (A375 cells: 24.9 ± 1.3; BCC cells: 25.1 ± 4.7). However, DAS and DADS failed to alter Ca^{2+} mobilization at the same concentration. The results indicated that the levels of Ca^{2+} change in A375 and BCC cells to DATS had a similar pattern with the intracellular ROS generation. We also estimated the level of $\Delta\Psi m$, which presents the membrane integrity of the mitochondria and is therefore considered as an indicator of apoptosis induced by mitochondrial pathway. By staining with $DiOC_6$ and further analyzing by flow cytometry, the level of $\Delta\Psi m$ was evaluated by the intensity of fluorescence. We found that the $\Delta\Psi m$ levels of A375 and BCC cells were markedly decreased after 24 h of DATS treatment (**Figure 4C**).

DATS Caused Changes in DNA Damage Response, Cell Cycle Progression, and Apoptosis Related Proteins. As DATS showed much stronger effect on cancer inhibition than that of DAS and DADS, we employed DATS for further studies. Studies have shown that cell cycle arrest following oxidative DNA damage is linked to cytokinesis failure and cell death (*20*). To explore the effect of DATS on the expression of DNA damage responsive protein, we investigated the expressions of phospho-γ-H_2AX (p-H_2AX), phospho-p53 (p-p53), and p21. Also, G_2 checkpoint modulators such as Cdc25c, Wee 1 kinase, and Cdc2 were measured. As indicated in **Figure 5A**, the A375 and BCC cells were treated with 25 μM of DATS at different times before Western blot analysis. The results illustrated that A375 and BCC cells treated with DATS caused dramatic increase in p-H_2AX (Ser 139) levels as early as 3 h in a time-dependent manner and largely increased about 11.0−12.2-fold at 24 h as compared with that at 0 h. Furthermore, DATS increased the expression of p-p53 importantly and the expression level reached the maximum by 12 h. Densitometry of the immunoblot also revealed that DATS induced 3.0- and 2.2-fold of p21 protein in A375 and BCC cells respectively after 24 h of treatment, as compared to that of control at 0 h.

To explore the mechanisms of DATS induced DNA damage, p53-mediated cell cycle arrest, and the occurrence of apoptosis in both skin cancer cells, we studied the expression of downstream targets of p53 including G_2/M arrest associated proteins. **Figure 5B** showed that exposure to DATS decreased the expressions of Cdc25c and Cdc2 and increased the levels of Wee 1 and cyclin B_1 expression in a time-dependent manner. As described above, DATS resulted in significant accumulation of sub-G_1 population in A375 and BCC cells, suggesting that the occurrence of DNA degradation was induced by apoptosis. Subsequently, we examined the level of apoptosis-related proteins in DATS treated A375 and BCC cells. Caspase-9 and caspase-3, the hallmarks of apoptosis, were observed after 24 h of treatment, and cleavage-caspase-9 was first detected at 12 h. Moreover, activation of caspase-9 and caspase-3 were accompanied by the reduction of full-length PARP protein levels and the increase of cleaved PARP protein levels after the treatment of DATS (**Figure 5C**).

DISCUSSION

The global incidence of skin cancers is rising at an alarming rate. World Health Organization claims that one in three cancer cases are skin-related, presenting the worldwide importance of skin cancers. Evidence indicated that allyl sulfides, the bioactive sulfur metabolites in garlic, show the ability of growth inhibition

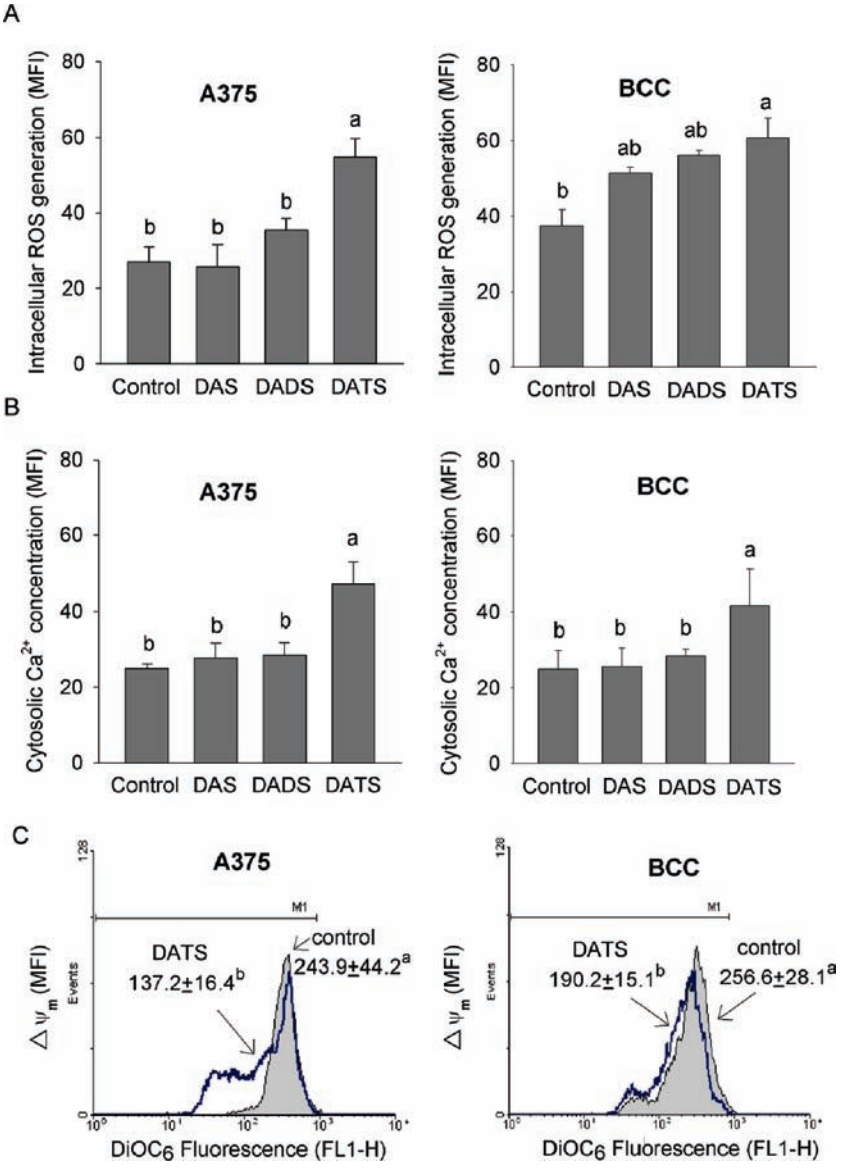

Figure 4. Estimation of intracellular ROS production, cytosolic Ca^{2+} concentration, and mitochondrial membrane potential ($\Delta\Psi_m$) in A375 and BCC cells. Cells were treated with 0.2% DMSO as control, and 25 μM of DAS, DADS, or DATS were treated for 1 h. Cells were harvested and assayed by carboxy-H_2DCFDA for ROS production determination (**A**) and Ca^{2+} concentration determination by Fluo-3/AM staining (**B**). In (**C**), cells were either treated with control or 25 μM of DATS for 24 h, then stained with $DiOC_6$ for $\Delta\Psi_m$ level determination described in Materials and Methods. Data presented the mean fluorescence intensity (MFI) mean ± SD of three determinations, and analyzed statistically using ANOVA and Duncan's test. Different letters (a−b) represent statistically significant differences among treatments, $p < 0.05$.

in several types of cancer cells (*10*). To our knowledge, the present study is the first report to demonstrate the putative mechanism mediated by DATS for controlling the growth of human skin cancer cells via DNA damage signaling pathway.

Here we illustrated that DATS, with stronger effects than DAS and DADS, could efficiently decrease the cell viability of A375 and BCC cells. This result was consistent with the previous finding that the number of sulfur atoms on allyl sulfides determines their anticancer activity (*9*, *18*). Although DAS did not have any effect on inhibiting cell viability at the dose of 25 μM after 24 h of treatment because its number of sulfur atoms was the lowest among the compounds used in this study. DAS exhibited cell growth control ability at either higher dose or longer duration treatment for 48 h in our unpublished data. Along with the specific effect on cancer cells, it reveals that the allyl sulfides in garlic extract have the potential in controlling the growth of skin cancer cells. We have shown here that the growth control ability of DATS might come from its G_2/M arrest and apoptosis inducing activity, which has been further improved by their molecular markers in parts **B** and **C** of **Figure 5**, respectively. It has been reported that DNA damage agents may trigger the arrest of cell cycle to exert DNA repair. After the renewal of DNA, cells might continue to have a normal cell cycle progression, while cells without proper repair undergo apoptosis (*19*). Because allyl sulfides have been demonstrated to induce DNA damage in cancer cells (*8*), we thus hypothesized that DATS might induce the cell cycle arrest and apoptosis via its role of being a DNA damaging agent. In agreement with our hypothesis, the expression of phospho-γ-H_2AX (p-H_2AX), an early signal of DNA damage, was detected at the early time point after DATS treatment and kept increasing throughout the times we measured. The results indicated that DATS inflicted DNA damage and thus elicited transient G_2/M arrest for DNA repair. Cells without complete DNA repair in our system might halt the chromosome

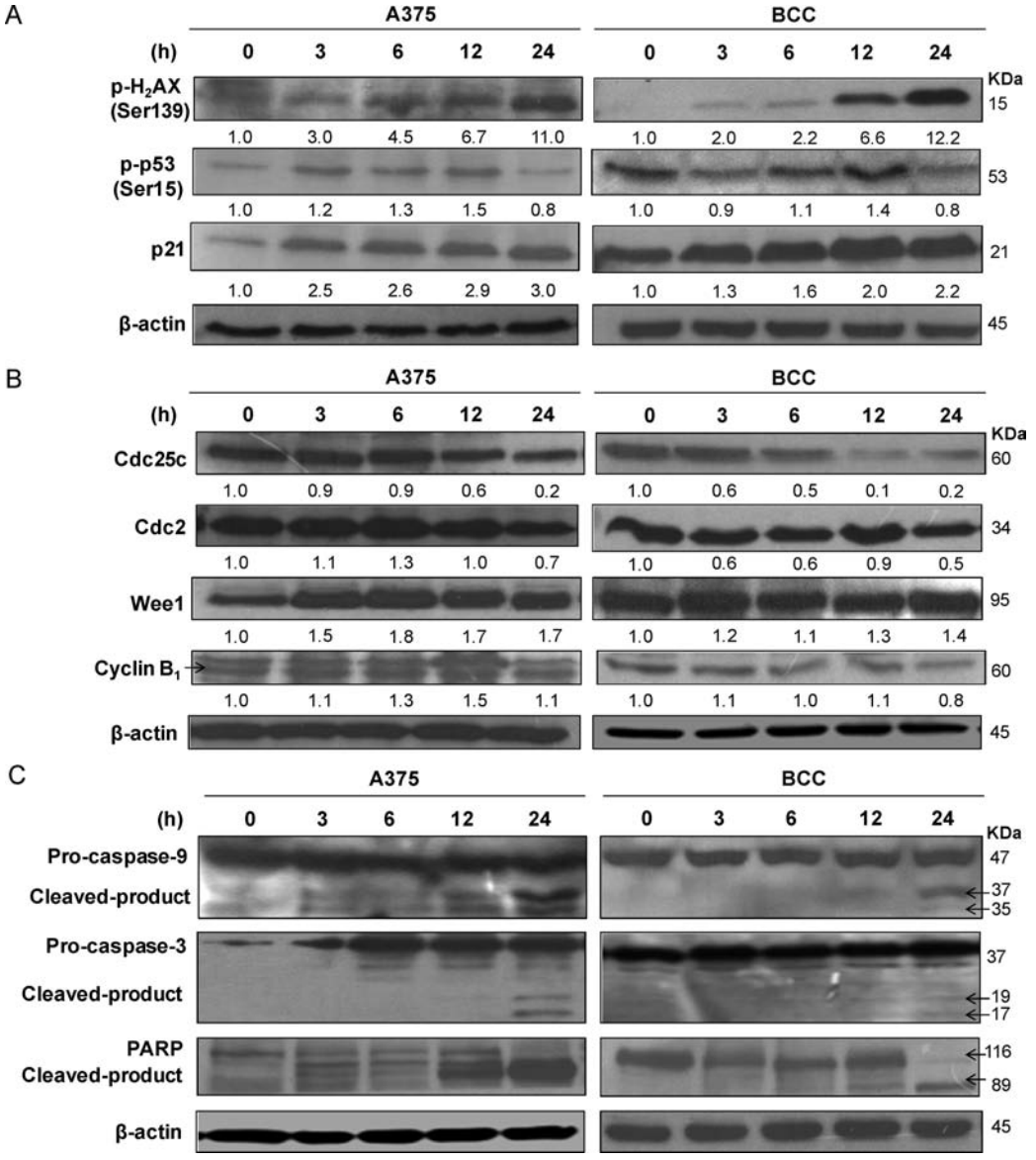

Figure 5. Expression change of certain proteins in A375 and BCC cells after the exposure to DATS. Cells were treated with 25 μM of DATS for different times and then the total cell lysates were prepared for Western blot analysis. The evaluation are followed by specific antibodies as the following (**A**) the protein levels of phospho-γ-H_2AX (Ser139), phospho-p53 (Ser15), and p21 protein; (**B**) the molecules involved in G_2/M transition such as Cdc25c, Wee l, Cdc2, and cyclin B_1 were detected; (**C**) the cleavage forms (pointed by the arrows) of apoptosis markers including caspase-9, caspase-3, and PARP were examined. Equal loading was confirmed by reprobing the membrane with β-actin in each analysis. Quantification of protein levels by β-actin-normalized densitometry was shown on bottom of each band.

segregation and cause the production of aberrant polyploidy DNA content as detected in cell cycle analysis. In accordance with the reports that the formation of polyploidy cell would lead to the cell death (*20*), we found that DATS caused a temporary G_2/M arrest, which was followed by an increasing percentage of polyploid DNA content and sub-G_1 DNA content by the cell cycle analysis at different time points. The apoptotic effects of DATS were confirmed by the increased level of cleaved caspase-9, cleaved caspase-3, and poly (ADP-ribose) polymerase (PARP), as well as disruption of mitochondrial membrane potential in this study.

Previous studies have shown that apoptosis induction is the possible mechanism of preventive effect of DAS in chemically induced mouse skin tumors (*17*). Moreover, increasing intracellular free calcium in human melanoma SK MEL-2 cells has been reported to the antiproliferative effect of DADS (*26*). A major finding of this study was to connect the modulation of ROS and cytosolic Ca^{2+} influx with the anticancer effects in skin cancer cells treated with DATS. We revealed that 25 μM of DATS increased intracellular ROS production and cytosolic Ca^{2+} mobilization as early as 1 h of treatment, which was earlier than the response of DATS induced cell cycle arrest and apoptosis. In addition, our unpublished data showed that the pretreatment of ROS scavenger *N*-acetyl cysteine (NAC) significantly suppressed DATS-induced ROS generation and cytotoxicity of A375 and BCC cells. These results corroborate with the previous studies (*27*), indicating that the production of ROS and Ca^{2+} are upstream factors for regulating the cell cycle. DATS is known to produce ROS by the homolytic cleavage of disulfide bonds, thus contributing to the pro-oxidant condition, such as protein thiolation and glutathione (GSH) depletion in cancer cells (*15*). Excessive physiological levels of ROS is regarded as the cellular DNA and protein damage agents (*28*). For example, inhibition of the spindle formation and disruption of cell division by DATS

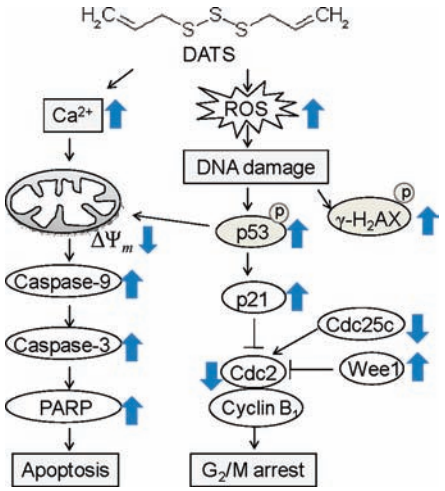

Figure 6. Proposed model of DATS induced cell cycle arrest and apoptosis in human melanoma A375 cells and BCC cells. The arrows indicated the expression changes in our results.

was resulted from its reactive sulfur atom, which contributed to the oxidation of cysteine residues in β-tubulin (*29*).

Interestingly, the expression of phospho-p53 (p-p53) and its downstream target p21 were induced after DATS treatment in both skin cancer cells. Studies have reported that A375 and BCC cells exhibit wild-type p53 function, which is activated during apoptosis induced by a variety of cellular stresses (*30*, *31*). P53 undergoes post-translational modifications and is stabilized and activated, leading to growth arrest and apoptosis of cells; consequently, damaged cells are prevented from further replication (*32*). The phosphorylation of serine 15 of p53 plays a role in responding to cellular DNA damage and the occurrence of p53-mediated apoptosis. Besides, DNA-damaging and proapoptotic multiple therapies were reported to alter the DNA status of tumor cells and regulate the protein expression of p53 (*33*). In this study, the serine 15 of p53 was phosphorylated at an early time point after DATS treatment, indicating that the activation of p53 happened soon after the occurrence of DNA damage. In parallel with the increase of functional p53, the expression of p53 downstream target p21, which was reported to be responsible for G_2/M arrest, was increased. Other than the up-regulation of cyclin dependent kinase inhibitor p21, the CDK1 (Cdc2)/cyclin B complex acting as the principal regulators determining G_2 to M transition or apoptosis was decreased by DATS. It is known that Cdc25c phosphatases and Wee 1 kinase play critical roles in maintaining G_2 phase arrest through modulating the phosphorylation of Cdc2 (*34*). We further revealed that DATS inhibited the levels of Cdc25c and Cdc2 but increased the levels of Wee 1 and cyclin B_1 in a time-dependent manner. The molecules we examined here explained the phenomenon of DATS induced G_2/M arrest. In addition to the induction of cell cycle arrest, p53 can trigger apoptosis related genes to affect the integrity of mitochondria and the consequent signaling for cell death (*32*). Taken together, we hypothesize that DATS triggered oxidative DNA damage and consequently induced G_2/M arrest and apoptosis through p53 pathway. It is well-known that p53 protein is one of the major targets to induce cell death and apoptosis for dermatological treatments. However, melanoma cells have low frequency of spontaneous apoptosis in vivo compared with the other tumor cell types and are relatively resistant to the compounds used in chemotherapy in vitro (*35*). Therefore, it is very important to develop a new therapeutic compound to trigger p53 mediated apoptosis in melanoma. Here we show the correlation of p53 activity and the growth inhibition of skin cancer cells, however, further studies are needed to demonstrate the role of p53 in DATS induced apoptosis and cell death in skin cancer cells. Additionally, our results showed that the growth inhibition of DATS was skin tumor cells specific and did not occur in normal cells. This finding is consistent with the previous studies in several cell types as well as in the animal studies (*36*). Nevertheless, the cause of the differential effect mediated by DATS between skin cancer cells and normal cells is still unclear. Our results suggest the possibility that ROS might play a critical role. It has been reported that compared to normal cells, ROS levels in certain cancer cells are realized to be close to the critical threshold for cell death (*12*).

In conclusion, we proposed the model of DATS induced G_2/M arrest and apoptosis in A375 and BCC skin cancer cells in **Figure 6**. DATS might increase the ROS level, and thus inflict DNA damage which could be detected by the phosphorylation of γ-H_2AX and the consequent activation of p53. p53 soon induces the expression of its downstream p21 and affects the G_2/M modulator such as Wee l kinase, Cdc25c, and Cdc2. Alternatively, p53 triggers the mitochondrial apoptotic pathway through the activation of caspase-9, caspase-3, and PARP.

It has been observed that oral administration of DATS inhibits the growth of cancer cells in human PC-3 prostate cancer xenografts in nude mice model without any harmful side effects (*36*). In agreement with the potential of DATS in the therapy potential for the other cell types, here we suggest that DATS exhibits preferable property of cancer preventive agents in skin cancer and also provides the possible mechanism for its anticancer effects.

ABBREVIATIONS USED

BCC, basal cell carcinoma; DAS, diallyl sulfide; DADS, diallyl disulfide; DATS, diallyl trisulfide; ER, endoplasmic reticulum; MFI, mean fluorescence intensity; MTT, 3-(4,5-dimethylthiazol-2-yl)-2,5-diphenyltetrazolium bromide; PARP, poly(ADP-ribose) polymerase; ROS, reactive oxygen species; $\Delta\Psi m$, mitochondrial membrane potential.

LITERATURE CITED

(1) Leiter, U.; Garbe, C. Epidemiology of melanoma and nonmelanoma skin cancer—the role of sunlight. *Adv. Exp. Med. Biol.* **2008**, *624*, 89–103.

(2) American Cancer Society. Cancer Facts & Figures 2009. Atlanta: American Cancer Society, 2009.

(3) Ohtsuka, H.; Nagamatsu, S. Changing trends in the number of deaths from nonmelanoma skin cancer in Japan, 1955−2000. *Dermatology* **2005**, *210*, 206–210.

(4) Cancer Registry Annual Report in Taiwan Area, 2006. Department of Health. The Executive Yuan: ROC, 2006.

(5) Soufir, N.; Basset-Seguin, N. Skin carcinogenesis. *Rev. Prat.* **1999**, *49*, 813–817.

(6) Cummins, D. L.; Cummins, J. M.; Pantle, H.; Silverman, M. A.; Leonard, A. L.; Chanmugam, A. Cutaneous malignant melanoma. *Mayo Clin. Proc.* **2006**, *81*, 500–507.

(7) Kim, J. Y.; Kwon, O. Garlic intake and cancer risk: an analysis using the Food and Drug Administration's evidence-based review system for the scientific evaluation of health claims. *Am. J. Clin. Nutr.* **2009**, *89*, 257–264.

(8) Yang, J. S.; Chen, G. W.; Hsia, T. C.; Ho, H. C.; Ho, C. C.; Lin, M. W.; Lin, S. S.; Yeh, R. D.; Ip, S. W.; Lu, H. F.; Chung, J. G. Diallyl disulfide induces apoptosis in human colon cancer cell line (COLO 205) through the induction of reactive oxygen species, endoplasmic reticulum stress, caspases casade and mitochondrial-dependent pathways. *Food Chem. Toxicol.* **2009**, *47*, 171–179.

(9) Wu, C. C.; Chung, J. G.; Tsai, S. J.; Yang, J. H.; Sheen, L. Y. Differential effects of allyl sulfides from garlic essential oil on cell

cycle regulation in human liver tumor cells. *Food Chem. Toxicol.* **2004**, *42*, 1937–1947.
(10) Powolny, A. A.; Singh, S. V. Multitargeted prevention and therapy of cancer by diallyl trisulfide and related *Allium* vegetable-derived organosulfur compounds. *Cancer Lett.* **2008**, *269*, 305–314.
(11) Lawson, L. D.; Wood, S. G.; Hughes, B. G. HPLC analysis of allicin and other thiosulfinates in garlic clove homogenates. *Planta Med.* **1991**, *57*, 263–270.
(12) Munchberg, U.; Anwar, A.; Mecklenburg, S.; Jacob, C. Polysulfides as biologically active ingredients of garlic. *Org. Biomol. Chem.* **2007**, *5*, 1505–1518.
(13) Liu, K. L.; Chen, H. W.; Wang, R. Y.; Lei, Y. P.; Sheen, L. Y.; Lii, C. K. DATS reduces LPS-induced iNOS expression, NO production, oxidative stress, and NF-kappaB activation in RAW 264.7 macrophages. *J. Agric. Food Chem.* **2006**, *54*, 3472–3478.
(14) Druesne-Pecollo, N.; Pagniez, A.; Thomas, M.; Cherbuy, C.; Duee, P. H.; Martel, P.; Chaumontet, C. Diallyl disulfide increases CDKN1A promoter-associated histone acetylation in human colon tumor cell lines. *J. Agric. Food Chem.* **2006**, *54*, 7503–7507.
(15) Filomeni, G.; Rotilio, G.; Ciriolo, M. R. Molecular transduction mechanisms of the redox network underlying the antiproliferative effects of allyl compounds from garlic. *J. Nutr.* **2008**, *138*, 2053–2057.
(16) Khan, A.; Shukla, Y.; Kalra, N.; Alam, M.; Ahmad, M. G.; Hakim, S. R.; Owais, M. Potential of diallyl sulfide bearing pH-sensitive liposomes in chemoprevention against DMBA-induced skin papilloma. *Mol. Med.* **2007**, *13*, 443–451.
(17) Arora, A.; Shukla, Y. Induction of apoptosis by diallyl sulfide in DMBA-induced mouse skin tumors. *Nutr. Cancer* **2002**, *44*, 89–94.
(18) Shrotriya, S.; Kundu, J. K.; Na, H. K.; Surh, Y. J. Diallyl trisulfide inhibits phorbol ester-induced tumor promotion, activation of AP-1, and expression of COX-2 in mouse skin by blocking JNK and Akt signaling. *Cancer Res.* **2010**, *70*, 1932–1940.
(19) Powell, S. N.; Bindra, R. S. Targeting the DNA damage response for cancer therapy. *DNA Repair* (*Amsterdam*) **2009**, *8*, 1153–1165.
(20) Varmark, H.; Sparks, C. A.; Nordberg, J. J.; Koppetsch, B. S.; Theurkauf, W. E. DNA damage-induced cell death is enhanced by progression through mitosis. *Cell Cycle* **2009**, *8*, 2951–2963.
(21) Mosmann, T. Rapid colorimetric assay for cellular growth and survival: application to proliferation and cytotoxicity assays. *J. Immunol. Methods* **1983**, *65*, 55–63.
(22) Wallen, C. A.; Higashikubo, R.; Dethlefsen, L. A. Comparison of two flow cytometric assays for cellular RNA—acridine orange and propidium iodide. *Cytometry* **1982**, *3*, 155–160.
(23) Zachwieja, J.; Zaniew, M.; Bobkowski, W.; Stefaniak, E.; Warzywoda, A.; Ostalska-Nowicka, D.; Dobrowolska-Zachwieja, A.; Lewandowska-Stachowiak, M.; Siwinska, A. Beneficial in vitro effect of *N*-acetyl-cysteine on oxidative stress and apoptosis. *Pediatr. Nephrol.* **2005**, *20*, 725–731.
(24) Bradford, M. M. A rapid and sensitive method for the quantitation of microgram quantities of protein utilizing the principle of protein−dye binding. *Anal. Biochem.* **1976**, *72*, 248–254.
(25) Puzianowska-Kuznicka, M.; Kuznicki, J. The ER and ageing II: calcium homeostasis. *Ageing Res. Rev.* **2009**, *8*, 160–172.
(26) Sundaram, S. G.; Milner, J. A. Diallyl disulfide inhibits the proliferation of human tumor cells in culture. *Biochim. Biophys. Acta* **1996**, *1315*, 15–20.
(27) Kim, Y. A.; Xiao, D.; Xiao, H.; Powolny, A. A.; Lew, K. L.; Reilly, M. L.; Zeng, Y.; Wang, Z.; Singh, S. V. Mitochondria-mediated apoptosis by diallyl trisulfide in human prostate cancer cells is associated with generation of reactive oxygen species and regulated by Bax/Bak. *Mol. Cancer Ther.* **2007**, *6*, 1599–1609.
(28) Passos, J. F.; Saretzki, G.; von Zglinicki, T. DNA damage in telomeres and mitochondria during cellular senescence: is there a connection? *Nucleic Acids Res.* **2007**, *35*, 7505–7513.
(29) Seki, T.; Hosono, T.; Hosono-Fukao, T.; Inada, K.; Tanaka, R.; Ogihara, J.; Ariga, T. Anticancer effects of diallyl trisulfide derived from garlic. *Asian Pac. J. Clin. Nutr.* **2008**, *17* (Suppl 1), 249–252.
(30) Jee, S. H.; Shen, S. C.; Tseng, C. R.; Chiu, H. C.; Kuo, M. L. Curcumin induces a p53-dependent apoptosis in human basal cell carcinoma cells. *J. Invest. Dermatol.* **1998**, *111*, 656–661.
(31) Koblish, H. K.; Zhao, S.; Franks, C. F.; Donatelli, R. R.; Tominovich, R. M.; LaFrance, L. V.; Leonard, K. A.; Gushue, J. M.; Parks, D. J.; Calvo, R. R.; Milkiewicz, K. L.; Marugan, J. J.; Raboisson, P.; Cummings, M. D.; Grasberger, B. L.; Johnson, D. L.; Lu, T.; Molloy, C. J.; Maroney, A. C. Benzodiazepinedione inhibitors of the Hdm2:p53 complex suppress human tumor cell proliferation in vitro and sensitize tumors to doxorubicin in vivo. *Mol. Cancer Ther.* **2006**, *5*, 160–169.
(32) Vogelstein, B.; Lane, D.; Levine, A. J. Surfing the p53 network. *Nature* **2000**, *408*, 307–310.
(33) Mroz, R. M.; Holownia, A.; Chyczewska, E.; Chyczewski, L.; Braszko, J. J. p53 N-terminal Ser-15 approximately P and Ser-20 approximately P levels in squamous cell lung cancer after radio/chemotherapy. *Am. J. Respir. Cell Mol. Biol.* **2004**, *30*, 564–568.
(34) Stanford, J. S.; Ruderman, J. V. Changes in regulatory phosphorylation of Cdc25C Ser287 and Wee1 Ser549 during normal cell cycle progression and checkpoint arrests. *Mol. Biol. Cell* **2005**, *16*, 5749–5760.
(35) Johnson, J.; Lagowski, J.; Sundberg, A.; Kulesz-Martin, M. P53 family activities in development and cancer: relationship to melanocyte and keratinocyte carcinogenesis. *J. Invest. Dermatol.* **2005**, *125*, 857–864.
(36) Xiao, D.; Lew, K. L.; Kim, Y. A.; Zeng, Y.; Hahm, E. R.; Dhir, R.; Singh, S. V. Diallyl trisulfide suppresses growth of PC-3 human prostate cancer xenograft in vivo in association with Bax and Bak induction. *Clin. Cancer Res.* **2006**, *12*, 6836–6843.

Received for review February 12, 2010. Revised manuscript received April 20, 2010. Accepted April 20, 2010. This study was supported by grant the NSC 98-2313-B-241-004 from the National Science Council, Taiwan, ROC.